Clumping in Hot Star Winds
W.-R. Hamann, A. Feldmeier & L.M. Oskinova, eds.
Potsdam: Univ.-Verl., 2008
URN: http://nbn-resolving.de/urn:nbn:de:kobv:517-opus-13981

Hydrodynamic simulations of clumps

A. Feldmeier, W.-R. Hamann, D. Rätzel & L. M. Oskinova
Universität Potsdam, Germany

Clumps in hot star winds can originate from shock compression due to the line driven instability. One-dimensional hydrodynamic simulations reveal a radial wind structure consisting of highly compressed shells separated by voids, and colliding with fast clouds. Two-dimensional simulations are still largely missing, despite first attempts. Clumpiness dramatically affects the radiative transfer and thus all wind diagnostics in the UV, optical, and in X-rays. The microturbulence approximation applied hitherto is currently superseded by a more sophisticated radiative transfer in stochastic media. Besides clumps, i.e. jumps in the density stratification, so-called kinks in the velocity law, i.e. jumps in $\mathrm{d}v/\mathrm{d}r$, play an eminent role in hot star winds. Kinks are a new type of radiative-acoustic shock, and propagate at super-Abbottic speed.

1 Line Driven Instability in 1-D

Clumps in hot star winds can be created by shock compression, where the shocks occur as result of the line driven instability, as first suggested by Lucy & Solomon (1970). First numerical simulations of this process were presented in a seminal paper by Owocki et al. (1988), and became possible through two novel "inventions": (1) The introduction of an exponential cutoff in the CAK (1975) power law distribution of line opacities. Perturbation growth through the line driven instability only terminates when highly accelerated gas is optically thin even in the strongest line transitions. Without an opacity cutoff, the instability-induced gas acceleration and rarefaction cannot be handled numerically. (2) The introduction of a photospheric Schuster-Schwarzschild reversing layer that allows for self-absorption in spectral lines via an inner boundary condition. Without this devise, the instability disrupts the flow already at the inner boundary. Owocki et al. (1988) treated only pure line absorption, but this shortcoming was overcome with the smooth source function method (SSF, Owocki 1991). This method is extensively reviewed in the literature (e.g. Owocki & Puls 1996), and is therefore not further discussed here.

The flow structure resulting from the line driven instability is shown in Fig. 1. (1) The instability steepens the velocity field of the wind on a macroscopic scale of order R_*. The basic action of the instability is to amplify positive velocity perturbations, in a cycle $\delta v \rightarrow -\delta\tau \rightarrow \delta F \rightarrow \delta g_l \rightarrow \delta v$ (with radiative flux F, and line force g_l). In words: a positive velocity perturbation Doppler-shifts a gas parcel out of the absorption shadow of gas lying closer to the star. The optical depth towards the parcel drops, the parcel experiences a stronger radiative flux from the star, and thus a larger line force, which *further* increases the velocity perturbation. (2) The highly accelerated and rarefied gas streams are decelerated in strong reverse shocks, by overdense shells. Due to the deceleration, the shells have a negative velocity gradient, and are no longer subject to the instability (Martens 1979). Ahead of the shells resides gas close to the stationary CAK density and velocity of the wind, however with negative velocity perturbations and again not subject to the instability. This gas acts as reservoir for the rarefied gas stream hitting the next outer shell. (3) From the outer rim of this reservoir, lumps of gas at CAK densities are ablated and radiatively accelerated through the almost void intershell space, until they hit the next outer shell, causing detectable X-ray emission (Feldmeier et al. 1997). X-ray emission from hot stars is covered in the contributions by Cassinelli et al., Oskinova et al., Cohen et al., and Leutenegger et al., in these proceedings. The gas reservoir is exhausted at around $7\,R_*$, and X-ray emission ceases. Figure 2 shows clumps propagating through void intershell space in snapshots from a numerical simulation.

This sequence of rarefied gas upstream of a dense shell, of the shell itself, and of a gas reservoir at CAK densities downstream of the shell can also be understood as one cycle of a radiative-acoustic Abbott wave. Initially, this is a harmonic wave, which then undergoes nonlinear deformation. This corresponds to the solution of Burgers' equation (that describes the kinematics of fast gas overtaking slow gas), where accelerating regions become ever broader in course of time, and decelerating regions become ever narrower, eventually turning into shock transitions. Since numerical simulations of the line driven instability do not adopt the Sobolev approximation, this is another hint that Abbott waves are not an artefact of the latter, as is occasionally uttered. Similarly, the line driven instability can be understood in the context of the Sobolev approximation, if second order terms including the curvature of the velocity

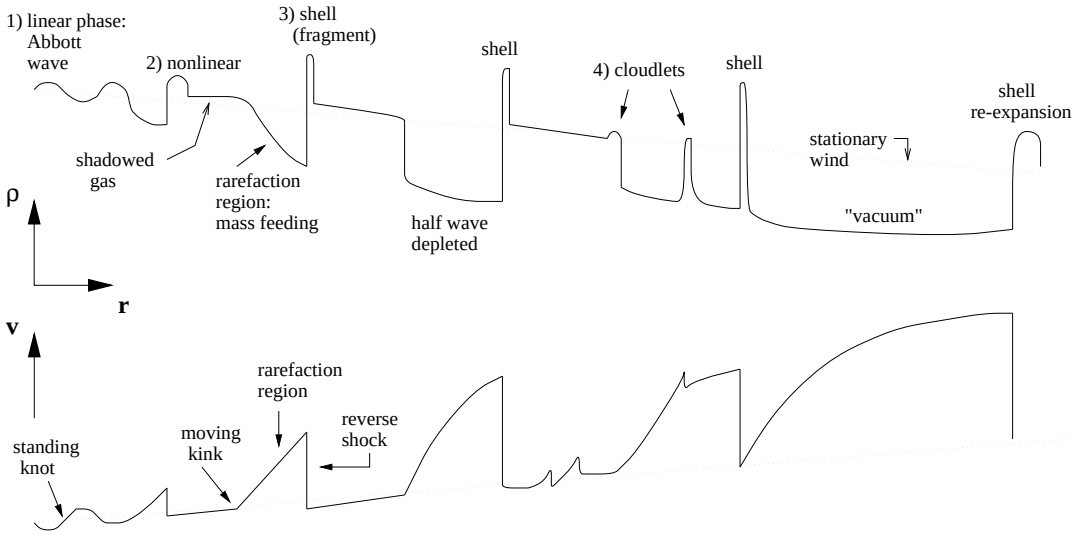

Figure 1: Radial wind structure that develops from the line driven instability.

field are included (Feldmeier 1998), and is then given by the cycle $\delta v \rightarrow \delta v'' \rightarrow -\delta\tau \rightarrow \delta F \rightarrow \delta g_l \rightarrow \delta v$ (with $v'' = \partial^2 v/\partial r^2$). In words: a positive velocity perturbation, or an elevation of the thermal band, increases the absolute curvature of the velocity field. By this, the Sobolev optical depth decreases (a second-order effect), the stellar radiative flux and the line force increase, and the velocity perturbation is further amplified.

2 Line Driven Instability in 2-D

In 1-D simulations assuming spherical symmetry, all flow structures correspond to shells. A key question is that for the real lateral scale of wind structure. Two basic scenarios are plausible: the Rayleigh-Taylor instability could fragmentize extended shell-like structures via eddies or fingers; and the line driven instability could amplify photospheric seed perturbations that have ab initio tiny lateral scale. This question is not decided yet. Another open question is whether the wind structure is essentially isotropic or not. X-ray line profiles look different for spherical (Owocki & Cohen 2006) and pancake-shaped, aligned absorbers (Feldmeier et al. 2003). However, due to the large number of model assumptions and free parameters in X-ray fitting, the data do so far not allow to make a conclusive decision.

Figure 3 shows a hypothetical sketch of the expected 2-D structure of an O star winds. At low and intermediate radii (out to a few stellar radii), three compression levels can be distinguished: (1) typical CAK densities, (2) shock compression one or two orders of magnitude above the CAK density, resulting from the line-driven instability, and (3) essentially void regions. As mentioned before, the gas (1) at CAK densities is ablated in form of small clumps from extended gas reservoirs directly above the dense shells, and the clumps are accelerated through void intershell regions (3), until they collide with the next outer shell (2), creating an observable X-ray flash. The gas reservoir (1) should be depleted by about seven stellar radii. The role of the void regions (3) in allowing X-rays to escape from the wind is discussed in Feldmeier et al. (2003, wind fragmentation) and Owocki & Cohen (2006, wind porosity).

At present, the only 2-D wind simulations of the line driven instability are by Dessart & Owocki (2003, 2005). In their first paper, a purely radial radiative force is assumed. The resulting wind structure is laterally incoherent, i.e. neighboring wind cones are completely independent. The question is whether lateral photons can cause some "lateral organization" of the flow. In their second paper, Dessart & Owocki used a tailored spatial mesh on which the single lateral photon ray considered crosses cell corners i, j and $i \pm 1, j \pm 1$, in order to minimize extrapolations. Models with high radial resolution show then indeed a high degree of lateral coherence. More specifically, the shells created by the line driven instability do *not* break up into clumps. However, the tailored mesh itself poses problems: in order that the photon ray hits cell corners as specified above, the radial mesh distance has to grow very fast with radius, which causes strong artificial dispersion of instability-generated structure.

We have recently started to program a short characteristics method for 2-D radiation hydrodynamics on a standard spatial mesh. An advantage of using short characteristics within the SSF approach

is that the latter only requires a high-precision calculation of optical depths, whereas for the intensity and source function rather simplified expressions are sufficient. Parabolic interpolation of intensity, which is often cumbersome in the short characteristics approach, can then be replaced by linear interpolation of optical depth, which has to be performed in the comoving frame however.

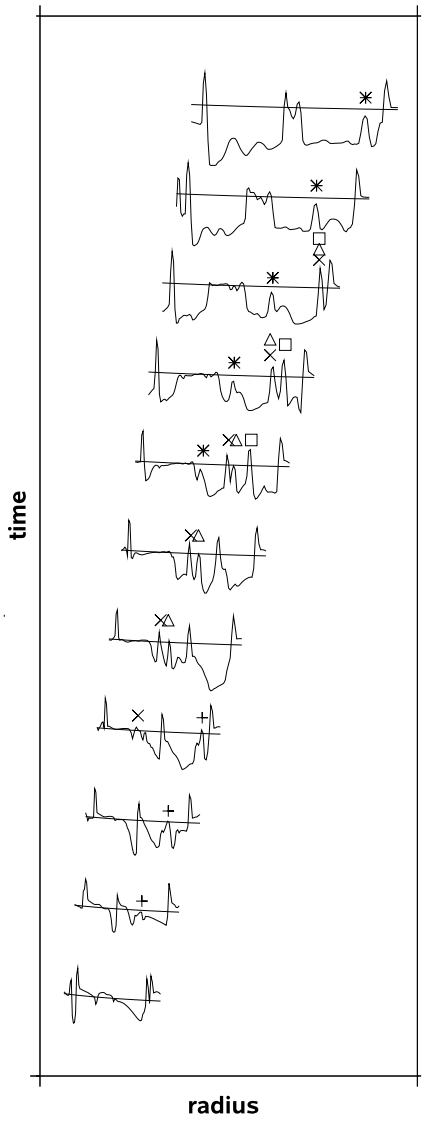

Figure 2: Clouds (marked $+$, $\times$, $\triangle$, $\square$, and $*$) are ablated from the gas reservoir ahead of a dense shell, propagate through a void region, and collide with the next outer shell.

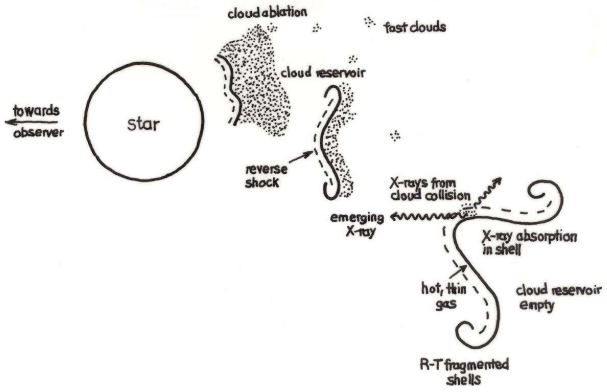

Figure 3: Sketch of wind structure expected from the line driven instability.

3 Multiple Radiative Resonances

If the velocity law of the wind is not monotonic, as is the case for clumpy winds, a photon can be absorbed in the same line transition at different loci. In the SSF approach, this is accounted for in the calculation of the total optical depth along a ray, but not in the calculation of the line source function. We have recently generalized an iteration method devised by Rybicki & Hummer (1978), to determine the line source function in presence of multiple resonances (Feldmeier & Nikutta 2006). Knowledge of the geometric shape of the resonance region is not required in this method, as the μ integral in the calculation of S is transformed to an r integral. A major problem of the method, however, which was not addressed by Rybicki & Hummer, is that "resonance caps," i.e. spherical fragments of finite angular size but tiny radial extent, can contribute significantly to the source function, while being badly resolved on a discrete radial mesh. We gave a remedy for this, and the lambda iteration proposed by Rybicki & Hummer converges then within a few iteration steps, if the number of resonance locations is small (three, in the above paper). This allows to calculate the source function at *each* time step of a hydrodynamic calculation on the *full* spatial mesh.

The method assumes validity of the Sobolev approximation in the calculation of the optical depth, whereas S is calculated via iteration as solution of the exact transfer equation. This is complementary to the SSF method, where τ is calculated (numerically) exact, whereas S is adopted from Sobolev approximation. It seems therefore natural and worthwhile to merge the two approaches in the near future.

4 Kink Propagation

Essentially all hydrodynamic simulations of hot star winds show the occurence of *kinks* in the velocity and density law of the wind. Kinks are discontinuities in the first spatial derivative of the wind speed or density, as opposed to shocks, which are discontinuities in the speed and density themselves. Kinks are found in overloaded or choked winds (Feldmeier & Shlosman 1999), in thin winds where metal ions and the H/He background plasma switch abruptly to a shallow solution branch in order to avoid decoupling (Krtiĉka & Kubát 2000), and in centrifugally-supported flows (Madura et al. 2007). Kinks are also thought to be connected to so-called discrete absorption components (DACs) observed in non-saturated P Cygni line profiles from OB stars. DACs could originate in an extended wind velocity plateau that termiantes in a kink (Cranmer & Owocki 1996): no clumping (i.e. density enhancement) is required to explain the "extra" absorption in a DAC. Still, outer wind clumps may be responsible for the formation of the extended velocity plateau and kink.

In standard hydrodynamics, kinks propagate at the sound speed. Similarly, Cranmer & Owocki suggest that the kink that terminates the velocity plateau should propagate upstream at the Abbott wave speed. The speed (in the stellar rest frame) at which the kink propagates away from the star is then (much) slower than the wind speed, and this would explain the observed slow frequency drift of DACs, which is roughly a factor of five smaller than expected from the wind acceleration.

The radiative force from line scattering in an optically thick gas parcel is proportional to the width of the frequency interval in which stellar radiative flux is intercepted, which in a strongly accelerating medium is proportional to the velocity shift $\mathrm{d}v$ across the parcel; and is inversely proportional to the mass of the parcel, which scales with its diameter $\mathrm{d}r$. Hence, the radiative force g_l scales with $\mathrm{d}v/\mathrm{d}r$ (not with v!). This leads to an interesting modification of the solution topology of line driven winds as compared to the solar wind and Laval nozzle flow. In the latter two cases, the critical or sonic point is a saddle point in the $r - v$ plane, whereas for line driven flows, the critical point is a saddle point in the $r - \mathrm{d}v/\mathrm{d}r$ plane (Bjorkman 1995). It is therefore not clear whether the concept of a *weak* discontinuity, i.e. a jump in the first spatial derivative of v and ρ that propagates at the sound speed, carries over from standard hydrodynamics to line driven flows. From analytical considerations we could recently show that radiative kinks propagate upstream at *super*-Abbottic speed (Feldmeier et al. 2008). Kinks or weak discontinuities in line driven flows behave therefore like *shocks* in standard gasdynamics, the shock being a strong discontinuity, i.e. a jump in v and ρ.

The essential argument is simple: the radiative or Abbott wave speed is given by $A = -\partial g_l/\partial v'$, and describes the response of the radiative force to perturbations of the velocity *gradient*. A careful treatment of the kink discontinuity leads to a kink speed $U = -[g_l]/[v']$ in the comoving frame, where the square bracket stands for the difference in a quantity across the kink. Since the CAK power law index is $\alpha < 1$, the function $g_l(v')$ at a given radius r is concave from below, hence the kink speed is faster than the Abbott speed. In this argument, $g_l(v')$ replaces the Hugoniot adiabate $p(\rho)$ from standard gasdynamics.

Regarding DACs in O star winds, this super-Abbottic upstream propagation of kinks causes an even slower outward propagation in the stellar rest frame then was assumed hitherto, which could further help to understand the slow evolution time of DACs.

5 Stochastic Transfer

The basic distinction between micro- and macroturbulence was introduced by Traving (1964): for microturbulence, hydrodynamic turbulence elements in a stellar atmosphere or the ISM are optically thin even at the center of a spectral line, and the turbulence is indistinguishable from thermal motion, and can be accounted for by a microturbulence velocity that is added to the thermal line broadening. For macroturbulence, on the other hand, a full line profile forms in every turbulence element, and one has to add these statistically independent, Doppler-shifted profiles to obtain the emergent line profile.

If the turbulent medium, or more generally any multi-phase medium, can be described statistically, i.e. if the density and velocity law are *random functions*, the radiative transfer has to be solved separately for each of the possible realizations of the medium, and the emergent intensity is obtained from averaging over all the realizations. This approach includes both the micro- and macroturbulence limit. In the microturbulence limit that the different phases cannot be distinguished from ordinary atoms by the photons, i.e. that the photon mean free path is much larger than the phase elements, the "averaging over realizations" can be replaced by a simpler "averaging over opacities", i.e. an effective opacity can be introduced, and the radiative transfer is solved once and for all on an "average" medium (e.g. filling factor approach).

By contrast, if the phase patches are *larger* than the photon mean free path, averaging of the emergent intensity over all realizations of the stochastic medium is unavoidable (e.g. in a Monte Carlo approach), since then $\langle e^{-\tau} \rangle \neq e^{-\langle \tau \rangle}$, where $\langle\, . \,\rangle$ indicates averaging. The latter inequality is readily understood, by writing out $\tau = \int \mathrm{d}\tau$, and expanding the exponential into a power series. The left and right hand side are then only identical if all n-point

correlation functions $\langle \mathrm{d}\tau(r_1)\mathrm{d}\tau(r_2)\ldots\mathrm{d}\tau(r_n)\rangle$ (with $r_1 < r_2 < \ldots < r_n$) are zero. But this is only true in the microturbulence or "atomic mix" limit that the clump size is smaller than the photon mean free path.

The calculation of n-point correlation functions is the biggest challenge of hydrodynamic turbulence theory, since (by definition) there are always large-scale eddies in hydrodynamic turbulence that cause large distance correlations, thus preventing n-point correlation functions from vanishing. Similarly, the radiation field that emerges from a medium with large-scale clumps obviously carries information about the stochastic properties of this medium, e.g. of the size distribution (power law vs. exponential) of the clumps.

Transfer theory in stochastic media was developed since the 1950ies (theory of Poisson processes), with applications e.g. to neutron transport in nuclear reactor walls. A modern landmark paper is Levermore et al. (1986), which demonstrates the mathematical complexity involved. The authors solve the "formal" transfer problem (pre-specified source function $S = B$) in a two-phase Markovian mix fully analytically. We quote here only a limiting case, for a medium that consists of infinitely dense absorbers in a background vacuum. For pure absorption ($S = 0$), the emergent intensity is then $I = I_0 \exp(-z/h)$, where h is the mean free path between the absorbers. This is the result for a fully *porous* wind, with porosity length h (see Hamann et al., Owocki et al., and Cohen et al., these proceedings).

A novel way to describe properties of stochastic media is via *percolation theory* (see reviews by Isichenko 1992 and Stauffer & Aharony 1992), which considers *stochastic clusters* in space, and transport upon them. Indelman & Abramovich (1994) derive an expression for the opacity of a two-phase medium via percolation theory. Their result is used to determine the degree of polution of rivers and lakes, and is used by Shaviv (1998) in a model for the inhomogeneous atmosphere of η Car. In its simplest form, percolation theory deals with two- and three dimensional, infinite grids, on which each position is either "filled" or "empty". When nearest-neighbor points are "filled", one speaks of a connection (which could mean e.g. that a current or heat flows). A celebrated result from percolation theory is that above a well-defined critical value for the space density of filled positions, the so-called percolation threshold, there exists one single-connected structure on the grid. Because of the long-range correlations near the percolation threshold, the latter is a *phase* transition. This explains the large interest in percolation theory in the settings of statistical mechanics.

The distinction between diffusion theory and percolation theory is, according to Broadbent & Hammersley (1957), that diffusion theory describes the stochastic motion (random walk) of a particle through a regular, ordered medium, whereas percolation theory describes an ordered, macroscopic motion (hydrodynamic fluid or electrical current) in a random medium. Diffusion theory was successfully applied by Ruszkowski & Begelman (2003) to describe the angular dependence of the radiation intensity in a medium with strong density contrasts, as in atmospheres of stars or accretion disks near the Eddington limit.

References

Bjorkman J.E. 1995, ApJ, 453, 369
Broadbent S.R. & Hammersley J.M. 1957, Proc. Cambridge. Philos. Soc., 53, 629
Castor J.I., Abbott D.C., & Klein R. 1975, ApJ, 195, 157 (CAK)
Cranmer S.R. & Owocki S.P. 1996, ApJ, 462, 469
Dessart L. & Owocki S.P. 2003, A&A, 406, L1
Dessart L. & Owocki S.P. 2005, A&A, 437, 657
Feldmeier A. 1998, A&A, 332, 245
Feldmeier A. & Shlosman I. 1999, ApJ, 526, 344
Feldmeier A. & Nikutta R. 2006, A&A, 446, 661
Feldmeier A., Puls J., & Pauldrach A. 1997, A&A, 322, 878
Feldmeier A., Oskinova L., & Hamann W.-R. 2003, A&A, 403, 217
Feldmeier A., Rätzel D., & Owocki S.P. 2008, ApJ, in print
Indelman P. & Abramovich B. 1994, Water Resources Research, 30, 3385
Isichenko M.B. 1992, Rev. Mod. Phys., 64, 961
Krtiĉka J. & Kubát J. 2000, A&A, 359, 983
Levermore C.D., Pomraning G.C., Sanzo D.L., & Wong J. 1986, J. Math. Phys., 27, 2526
Lucy L.B. & Solomon P.M. 1970, ApJ, 159, 879
Madura T.I., Owocki S.P., & Feldmeier A. 2007, ApJ, 660, 687
Martens P.C.H. 1979, A&A, 75, L7
Owocki S.P. 1991, in Stellar atmospheres: beyond classical models, eds. Crivellari L., Hubeny I., & Hummer D.G., Kluwer, Dordrecht, 235
Owocki S.P. & Puls J. 1996, ApJ, 462, 894
Owocki S.P. & Cohen D.H. 2006, ApJ, 648, 565
Owocki S.P., Castor J.I., & Rybicki G.B. 1988, ApJ, 335, 914
Ruszkowski M. & Begelman M.C. 2003, ApJ, 586, 384
Rybicki G.B. & Hummer D.G. 1978, ApJ, 219, 654
Shaviv N.J. 1998, ApJ, 494, L193
Stauffer D. & Aharony A. 1992, Introduction to Percolation Theory, Taylor & Francis, London
Traving G. 1964, Zeitschrift f. Astrophysik, 60, 167